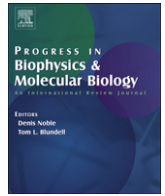


Contents lists available at [SciVerse ScienceDirect](http://www.sciencedirect.com)

Progress in Biophysics and Molecular Biology

journal homepage: www.elsevier.com/locate/pbiomolbio

Original research

Perturbed voltage-gated channel activity in perturbed bilayers: Implications for ectopic arrhythmias arising from damaged membrane

Catherine E. Morris^a, Peter F. Juranka^a, Béla Joós^{b,*}^a OHRI, Ottawa, ON, Canada^b Department of Physics, University of Ottawa, Ottawa, ON, Canada

ARTICLE INFO

Article history:

Available online xxx

Keywords:

Voltage gated channels
Mechanosensitivity
Membrane tension
Blebs

ABSTRACT

The ceaseless opening and closing of the voltage-gated channels (VGCs) underlying cardiac rhythmicity is controlled, in each VGC, by four mobile voltage sensors embedded in bilayer. Every action potential necessitates extensive packing/repacking of voltage sensor domains with adjacent interacting lipid molecules. This renders VGC activity mechanosensitive (MS), i.e., energetically sensitive to the bilayer's mechanical state. Irreversible perturbations of sarcolemmal bilayer such as those associated with ischemia, reperfusion, inflammation, cortical-cytoskeleton abnormalities, bilayer-disrupting toxins, diet aberrations, etc, should therefore perturb VGC activity. Disordered/fluidized bilayer states that facilitate voltage sensor repacking, and thus make VGC opening too easy could, therefore, explain VGC-leakiness in these conditions. To study this in membrane patches we impose mechanical blebbing injury during pipette aspiration-induced membrane stretch, a process that modulates VGC activity irreversibly (plastic regime) and then, eventually, reversibly (elastic regime). Because of differences in sensor-to-gate coupling among different VGCs, their responses to stretch fall into two major categories, MS-Speed, MS-Number, exemplified by Nav and Cav channels. For particular VGCs in perturbed bilayers, leak mechanisms depend on whether or not the rate-limiting voltage-dependent step is MS. Mode-switch transitions might also be mechanosensitive and thus play a role. Incorporated mathematically in axon models, plastic-regime Nav responses elicit ectopic firing behaviors typical of peripheral neuropathies. In cardiomyocytes with mild bleb damage, Nav and/or Cav leaks from irreversible MS modulation (MS-Speed, MS-Number, respectively) could, similarly, foster ectopic arrhythmias. Where pathologically leaky VGCs reside in damaged bilayer, peri-channel bilayer disorder/fluidity conditions could be an important "target feature" for anti-arrhythmic VGC drugs.

© 2012 Elsevier Ltd. All rights reserved.

1. VGC activation is tuned by bilayer structure

Voltage-gated channels (VGCs) are mechanosensitive (MS) integral membrane proteins (Schmidt and MacKinnon, 2008; Morris and Juranka, 2007b; Morris, 2011b). Their probability of being open (P_{open}), though primarily a function of V_m (membrane voltage), is unavoidably modulated by the variable mechanical states of the bilayers in which they are embedded. When V_m changes, a VGC's four positively-charged and peripherally-located voltage sensors "repack" relative to the channel's central pore. As they repack, the sensors pull at gate regions. If the gate opens, ions flow through the central pore (Yifrach and MacKinnon, 2002; Krepley et al., 2009). The ease and hence speed of voltage sensor repacking varies with the structural specifics of the embedding

lipid bilayer, whose molecules must, themselves, repack to accommodate voltage sensor repacking. Whether transient or sustained, reversible or irreversible, therefore, perturbations of bilayer structure will perturb sensor motions. The mutual rearrangements of sensor domains and lipid molecules occur more easily in highly fluidized disorderly ("softer") bilayers and with more difficulty in highly ordered ("stiffer") bilayers (for simple abiotic bilayers the terms would be liquid-disordered versus liquid-ordered). Accordingly, for any VGC in its native setting, sensor activity is tuned by the mechanical state of the lipid matrix.

Before discussing how, for different VGCs, perturbed bilayer/sensor interactions result in two categories of MS modulation – MS-Speed and MS-Number – (summarized in Fig. 1), we illustrate the perils of irreversible MS-modulation of VGC activity in excitable cells with damaged bilayer. The scenario: in mildly traumatized axons, voltage-gated sodium (Nav) channels trigger ectopic activity (Fig. 2). These simulated outcomes (Boucher et al., 2012) robustly show hallmark features of ectopic neuropathic

* Corresponding author.

E-mail address: bjjoos@uottawa.ca (B. Joós).

firing in peripheral neuropathies (Kovalsky et al., 2008). Previously, more complex and biophysically less well-justified models that require multiple Nav channel subtypes have been invoked to explain these behaviors. Cardiac arrhythmias originating from peri-infarct zones might similarly be initiated or exacerbated (Bouchard et al., 2011) by Nav, Cav, HCN and Kv channels (Du and Nathan, 2007; DiFrancesco and Borer, 2007; Moreno and Clancy, 2012; Mottram et al., 2011; Remme and Bezzina, 2010; Ganapathi et al., 2010) in mildly-damaged structurally-perturbed sarcolemmal bilayers. For the ultrastructure of extreme ischemia-related sarcolemmal damage, see Sage and Jennings (1988). If our view of dysfunctional excitability in sick excitable cells proves correct, then as we have argued in the context of amphiphilic Nav inhibitors and injured axons (Morris et al., 2012), renewed attention (see Mason (1993)) is warranted to the bilayer-partitioning attributes of amphiphilic VGC inhibitors. Ideally, drugs for blocking VGCs in such sick excitable cells could be designed to target the malfunctioning (leaky) channels by partitioning with greater avidity into fluidized, damaged bilayer than into healthy well-packed bilayer.

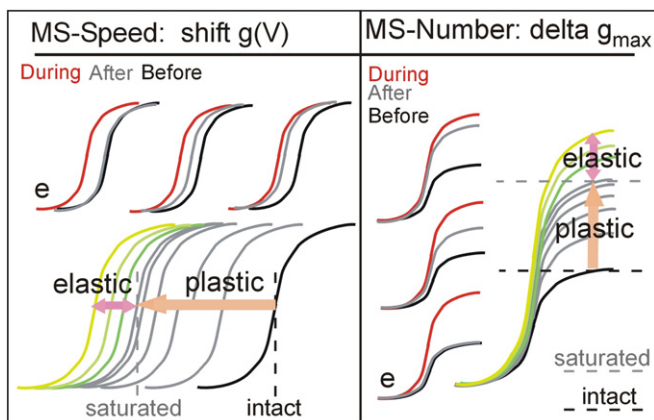


Fig. 1. VGC activation and membrane stretch: MS-Speed and MS-Number responses. MS-Speed: shifts along the V_m -axis. MS-Number: a change in the apparent g_{\max} . For stretch at a given intensity, changes in $g(V)$ can be fully reversible (marked with an e), partially reversible, or irreversible (before (black), during (red) and after stretch (gray)). In response to progressively increasing stretch intensity, $g(V)$ curves for VGCs for an initially intact membrane go through a range of irreversible changes (= the plastic regime). This saturates at some point. Thereafter, reversible stretch-intensity dependent changes can be recorded without interference (= elastic regime). Thus, for oocyte patches subjected to prolonged pipette aspiration (Morris et al., 2006), membrane damage constitutes the continuum of the states along the path between the initially intact plasma membrane and a fully blebbed membrane (see, eg. Zhang et al., 2000). The sigmoid-shaped curves represent activation Boltzmann relationships for voltage-dependent transitions (between two states) of the VGC. The midpoint, $V_{0.5}$, reflects the internal energy difference of the two states in the absence of voltage and the slope, i.e. voltage-sensitivity, reflects the effective charge that moves in association with the transition. To date, no cases have been reported in which voltage-sensitivity changes with stretch (Morris, 2011a). Instead, as per this sketch, the irreversible and reversible responses of VGCs to membrane deformations yield $V_{0.5}$ shifts or increased Boltzmann amplitudes. For VGCs like the VGCa and Kv3 channels, “ g_{\max} ” does not correspond to its Hodgkin–Huxley meaning (literally, 100% of channels open 100% of the time) since, experimentally-induced increases in “apparent g_{\max} ” are seen routinely (e.g. with drugs) and this is the characteristic response with stretch (see Calabrese et al. (2002), and Laitko et al. (2006)). When apparent g_{\max} changes, single channel recordings reveal possible contributions from changes in: unitary conductance, mean open time and/or the number of participating channels. For VGCa channels, increased numbers of participating channels is the best explanation, both for whole-cell inflation and cell-attached patch stretch (Calabrese et al., 2002). If a membrane patch develops a non-zero resting tension (Morris and Sigurdson, 1989; Suchyna et al., 2009), $V_{0.5}$ and apparent g_{\max} values for MS VGCs studied in patches may change. This makes it useful, when possible, to compare results for whole-cell inflation and patch stretch, as was done for VGCa channels, which showed good agreement (Calabrese et al., 2002).

2. Ectopic “pacemaking” and leaky Nav channels in damaged membrane

Nav channels can become leaky in many excitable membranes (see Table 1 in Morris et al., 2012), including Nav-rich myelinated axons (Wolf et al., 2001; Karoly et al., 2010; Schafer et al., 2009) subjected to insult (ischemia, reperfusion injury, inflammatory injury, trauma). “Sick cell Nav-leak” has usually been attributed exclusively to slow-mode Nav channels but we suggest that fast-mode channels too would contribute (Wang et al., 2009; Boucher et al., 2012). With Nav channels operating at $\sim 1\%$ slow-mode, 99% fast-mode, steady-state fast-mode current (=window current) is the dominant “persistent I_{Na} ” at voltages near firing threshold. Then, as V_m depolarizes through the window conductance region, slow-mode I_{Na} would dominate (Fig. 4D in Morris et al., 2012). Recombinant Nav1.6 behavior implicates both Nav channel modes in Nav-leak; we found (Wang et al., 2009; Morris et al., 2012) that with membrane injury, both slow- and fast-mode Nav channels undergo irreversible hyperpolarizing (left) shifts. If native g_{Na} behaves similarly, both modes will contribute to damage-induced Nav-leak, with fast-mode Nav channels activating at levels that, in a healthy cell, would be in the subthreshold V_m range (Boucher et al., in press; Morris et al., 2012).

Left-shifted activation curves ($g(V)$) (Fig. 1, MS-Speed panel; Fig. 2A) occur for Nav channels when voltage sensors move too easily in disordered, fluidized bilayers (Morris and Juranka, 2007a). Cardiomyocytes spend a larger fraction of time depolarized than do axons. Slow-mode g_{Na} would therefore normally contribute more to the persistent Na^+ influxes of cardiomyocytes (Mottram et al., 2011; Moreno and Clancy, 2012; Létienné et al., 2009; Weiss et al., 2010) than in axons. This would be all the more true where g_{Na} became left-shifted in the form of a sick-cell Nav-leak. This idea will need to be addressed experimentally and computationally. Our modeling of voltage-clamped slow and fast gating currents was simplified: co-existing non-inactivating and fast-inactivating g_{Na} without/with a 20 mV left-shift (Morris et al., 2012). The aim was simply to assess how experimenters could use sawtooth ramp clamp to help dissect fast/slow g_{Na} -leak sub-components during progressive mechanically-induced membrane damage, i.e., irreversible perturbation from the bleb-inducing process of pipette aspiration. More precise models involving kinetically interconnected slow- and fast-inactivating Nav channel states (e.g. Karoly et al., 2010) applied to healthy vs progressively shifted g_{Na} will be needed to guide experimental approaches and interpret data on cardiomyocyte pathophysiology and pharmacology.

To date, our excitable cell action potential computations on left-shift Nav-leak have been for axons. The particular goal was to assess the impact of the overlooked component – i.e., fast-mode Nav-leak. Fig. 2A and B illustrate $I_{Na}(t)$ data from Nav1.6 channels in oocyte membrane patches pre- and post-stretch (stretch is due to pipette-aspiration). Consistent with such data we devised a biophysically precise, yet computationally tractable model of fast-mode based Nav injury. Our Hodgkin–Huxley based injury model is Nav-CLS (CLS = “coupled left-shift”) (Boucher et al., 2012). When Nav fast-activation left-shifts, fast-inactivation (a voltage-independent process whose speed is limited by and thence coupled to activation) left-shifts by the same number of millivolts. Note that in Nav-CLS, when m^3 and h (gating parameters) left-shift by a given amount (a large shift, 20 mV, is shown in Fig. 2A top) the window conductance, $m^3h(V)$, necessarily left-shifts by that amount (bottom). Experimental traces in Fig. 2B are from a membrane whose stretch-induced injury by chance caused a precisely 20 mV left-shift of $g_{Na}(V)$.

An experimental footnote: injury intensity becomes evident post-hoc and cannot be precisely controlled as it is inflicted.

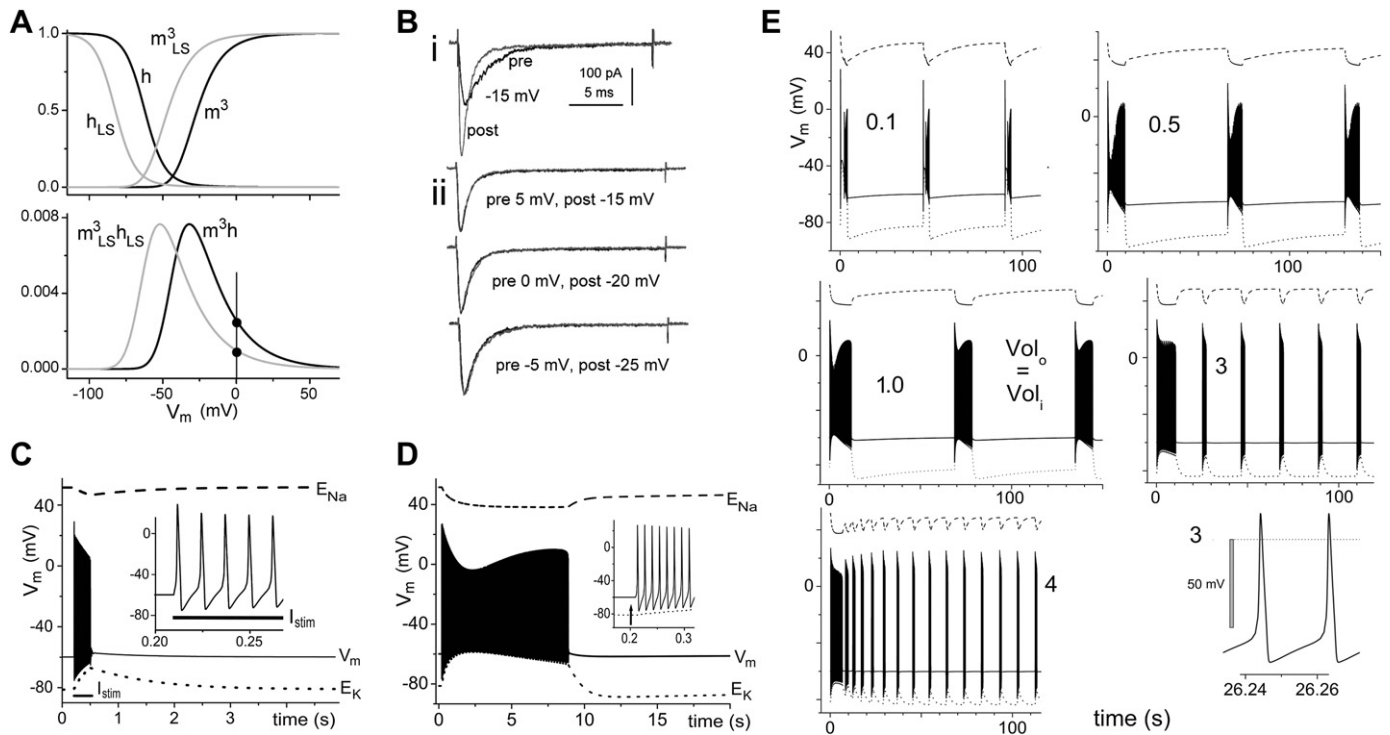


Fig. 2. Nav-CLS injury and ectopic excitation. A. Hodgkin–Huxley $m^3(V)$ and $h(V)$ plots for control conditions and with 20 mV hyperpolarizing (left) shifts; below, their steady-state products (window conductances). B. As explained in the text, i) irreversible response of recombinant Nav1.6 current to stretch, and ii) illustration of a 20 mV coupled left-shift. C, D, E. Computational results as described in the text. A few expanded insets show action potential shapes. C, intact axon. D, a mild axon trauma, 1.5 mV Nav-CLS. In E, the Nav-CLS injury (2 mV, all Nav channels) is identical for all simulations; only the ratio for vol_o/vol_i varies (0.1, 0.5, 1.0, 3 and 4).

For cell-attached patches (Morris et al., 2006) subjected to pipette aspiration (Sheetz et al., 2006), damage will fall along a continuum between the intact and fully blebbed plasma membrane (see, eg. Zhang et al., 2000; Suchyna et al., 2009). A bleb is a region of plasma membrane where the bilayer has dissociated from its previously adherent membrane cytoskeleton. Blebbing can be cell-mediated and tightly regulated (Charras and Paluch, 2008) or injury-induced and essentially irreversible (Armstrong et al., 2001; Morris, 2011a; Sage and Jennings, 1988). In the latter case blebbing gradually reduces the bilayer's normal lateral subdomain organization and its leaflet asymmetry. As the aspiration-induced damage intensifies, the original bilayer's far-from-equilibrium cell-mediated, ATP-dependent structure decays toward a high-entropy self-organized, essentially abiotic state (Morris, 2011a, 2011b, Morris et al., 2012; Zhang et al., 2000). For Nav-CLS injury, this injury continuum corresponds to the MS-Speed plastic regime in Fig. 1. As the pipette aspiration (blebbing) injury progressively takes an intact patch to a maximally injured condition (labeled “saturated” in the figure), the value of Nav-CLS (0 mV for intact membranes) can be as large as 35 or 40 mV (Tabarean et al., 1999; Wang et al., 2009; Beyder et al., 2010). Because of unintended seal-formation damage (see Morris et al., 2006; Wang et al., 2009; Zhang et al., 2000), the intentionally-imposed injury might not start from a true Nav-CLS = 0 mV. Fig. 2 Bi shows $I_{Na}(t)$ at $V_m = -15$ mV before and after (pre, post) stretch. Then, from that patch, Bii shows that peak-normalized $I_{Na}(t)$ traces overlap perfectly for pre-stretch at x mV, post-stretch at $(x - 20)$ mV (as labeled). Thus post-stretch- $I_{Na}(t)$ is kinetically equivalent to intact- $I_{Na}(t)$ 20 mV to the “left. This example therefore constitutes a 20 mV Nav-CLS injury.

In Nav-CLS injury, the shifted component of window current from a damaged region of membrane would essentially be a pathological version of subthreshold persistent I_{Na} (Boucher et al., in press). In pacemaking interneurons, fast-mode based subthreshold

persistent I_{Na} serves as a pacemaker current (Taddese and Bean, 2002), but for axons, pacemaking is anathema as it is too far, say, ventricular cardiomyocytes.

For Nav-CLS injury modeled in axons, we varied both the fraction of total g_{Na} affected and the injury intensity (Boucher et al., 2012). If one projects to cardiomyocytes our axon-model findings regarding ectopic firing, propagation block, and dysregulated ion homeostasis, it would suggest that damaged regions of cardiac sarcolemma (Post et al., 1988; Sage and Jennings, 1988) could cause comparable problems. Cardiac Nav1.6 (isoform in sinoatrial node cells, Lei et al., 2004) is certainly of interest, but the possibility of pathologic MS modulation of Nav1.5, the major cardiac isoform, is also worth pursuing. It is a candidate for Nav-CLS since a) stretch co-accelerates the (coupled) activation/fast-inactivation time courses of Nav1.5 (Morris and Juranka, 2007a; Banderali et al., 2010b) and b) in Nav1.5-expressing HEK cells, pipette aspiration causes large irreversible $g(V)$ left-shifts (Beyder et al., 2010).

For an “intact” Hodgkin–Huxley axon with Na/K pumps (internal and external volumes equal: $vol_o = vol_i$), Fig. 2C plots V_m , E_{Na} and E_K (Boucher et al., 2012). Prolonged current injection elicits sustained firing that stops when injection stops, after which the pump slowly readjusts the ion gradients. Within a few seconds the system has returned to its initial state. This, then, is the healthy axon's response to a long stimulus. Adjacent (Fig. 2D) is the same axon's response to a sudden mild injury. There is no stimulating current here; instead, at $t = 0.2$ s, a mild irreversible Nav-CLS injury is imposed (all Nav channels shifted by 1.5 mV). For more than 8 s, the previously quiescent axon fires tonically. Propagating antero- and retrogradely, this “spontaneous” ectopic firing would constitute a seriously neuropathic condition. Note that the mild Nav-CLS injury causes E_{Na} and E_K change due to channel activity. At a certain point, ectopic firing ceases and several seconds later the injured system has settled into a new steady-state. The axon's (ATP-

consuming) pumps have successfully responded to the small Nav-CLS injury, yielding a slightly hyperpolarized new value for E_K . When more intense and/or extensive Nav-CLS injury is imposed, the system's new steady-states are quasi-fixed V_{rest} values, but with slow rhythmic patterns of bursts, as seen, e.g. in the $vol_o = vol_i$ case of Fig. 2E. Other $V_m(t)$ simulations in that series demonstrate that bursting particulars change strikingly when the $vol_o:vol_i$ ratio is varied. This shows the importance, for excitability patterns, of system interactions between pump and Nav channel behaviors. Severe Nav-CLS injury (e.g., the 20 mV shift of Fig. 2A) yields depolarizing block, but even then, window current leak will dissipate the Na^+ -gradient. Importantly, subthreshold voltage oscillations, a common feature of neuropathic firing (Kovalsky et al., 2008), are a robust feature of mild Nav-CLS injury (Boucher et al., 2012; Yu et al., in press).

These results for an axon model serve as a heads-up that leaky fast-mode Nav gating in damaged cardiomyocyte (among other excitable cells) may have been overlooked. The clinical effectiveness of Nav reagents with higher binding affinity to slow-mode than fast-mode Nav channels is not proof that only slow-mode Nav-leak occurs (Lenkey et al., 2011; Karoly et al., 2010); in situ, these lipophilic agents might partition (Mason, 1993) better into damaged than intact bilayer (Morris et al., 2012). Our simulations show why inhibiting Kv channels or pumps or volume regulatory transporters (or, as we show, altering compartment volumes) would change the firing patterns (as per Fig. 2E) even when the underlying cause of the dysrhythmia was, in fact, Nav-CLS. If slow-mode Nav activity is mistakenly assumed to be the sole source of leak, the expectation is that in the g_{max} zone, steady-state I_{Na} will increase relative to peak I_{Na} . But relying on this assessment of persistent Nav leak would be misleading if some of the leak was due to Nav-CLS injury. In that case, the ratio of [steady-state I_{Na} at ~ 0 mV] to [peak I_{Na} at ~ 0 mV] will decrease (see the region near 0 mV in the $m^3h(V)$ plot of Fig. 2A).

The possibility of left-shifted slow-mode Nav channels (Morris et al., 2012) in mildly damaged cardiomyocyte membranes urgently needs to be investigated. Where there is slow-mode Nav-LS injury (see Morris et al. (2012)), there will also be fast-mode Nav-CLS injury: these channels constitute one population in different modes (see Fig. 1 of Morris et al. (2012) and see Karoly et al. (2010)).

3. Reversible and irreversible MS modulation of VGCs

Excitable cells can fine-tune their firing patterns by modulation of VGCs. In both healthy and diseased conditions restructuring (deforming) the embedding bilayer is one way to modulate VGCs. Morris (2011c) lists where/when, in the cardiac cells, one might expect mechanically-induced elastic bilayer deformations. Irreversible physiological or pathological changes in bilayer structures would also be bilayer mechanical perturbations. To study MS modulation of recombinant and native VGCs, we and others exploit stretch (Langton, 1993; Morris et al., 2006; Beyder et al., 2010) or patch excision (Schmidt and MacKinnon, 2008) or bilayer reagents. Cholesterol and fatty acids and various lipids or lipophilic compounds can be added/extracted (Finol-Urdaneta et al., 2010; Ganapathi et al., 2010; Shcherbatko et al., 1999; Du and Nathan, 2007; Li et al., 2009; Schmidt and MacKinnon, 2008; Schmidt et al., 2009). Bilayer-disrupting (Ali et al., 2010) drugs e.g. capsaicin (Bruno et al., 2007), propofol (Liu et al., 2011), thiazolidinediones (Rusinova et al., 2011) may be used; there the interest is largely clinical side effects (Morris and Juranka, 2007b) on VGCs. Hydrostatic pressure also deforms bilayers, compressing them laterally to yield thicker more ordered, densely-packed bilayers (Periasamy et al., 2009). This may explain (see Morris and Juranka (2007a)) how large hydrostatic pressures reversibly decelerate and right-shift the activation (coupled with

inactivation) of squid axon g_{Na} (Conti et al., 1982); originally, because voltage sensor motions were thought to be sequestered from the bilayer, those findings were interpreted strictly in terms of pressure-induced changes to the activation volume of a protein in an aqueous environment, neglecting the possibility of force-sensitive shape changes at the VGC's lateral interface with the bilayer. Like membranes under hydrostatic pressure, cholesterol/sphingomyelin-enriched membranes are thicker and more ordered (compared to cholesterol-extracted membranes), and this exerts hydrostatic pressure-like effects on Nav and Kv channel gating (slower, more right-shifted activation). Membrane stretch, by contrast, thins, fluidizes and disorders bilayers, eliciting in Nav and Kv1 channels faster, more left-shifted activation (see Morris and Juranka (2007b), Morris (2011b, 2011c)). And consistent with all this, for HCN2 channels (VGCs that deactivate rather than activate with depolarization), stretch reversibly accelerates deactivation (Lin et al., 2007). In effect, VGC responses to hydrostatic compression and tensile stretch seem to occupy a bilayer mechanical continuum.

The key issue here is the behaviors of VGCs in sick excitable cell membranes (Morris, 2011a; Morris et al., 2012) and in particular, in cardiomyocytes with damaged bilayers. Where bilayer/membrane–cytoskeleton interactions become disrupted (e.g. VanWinkle et al., 1994), bilayer disorder/fluidity is elevated and the bilayer's healthy asymmetry decays (a genetically-induced case occurs with dystrophic membranes (Allen et al., 2010; Hirn et al., 2008; Tuazon and Henderson, 2012)). This is bleb type injury, even though in mildly injured cells (the potentially salvageable ones) regions of nascent bleb may be too small and dispersed to be evident by light microscopy. Thus, for blebbing injuries in cardiomyocytes, the VGC-rich areas of greatest interest are not the late-stage blebs and vacuoles characteristic of apoptotic and necrotic post ischemia/reperfusion cells (Khanal et al., 2011; Sage and Jennings, 1988; VanWinkle et al., 1994), but membranes whose bilayer/actomyosin–spectrin adhesions are just beginning to fail. In porcine cardiomyocytes subjected to ischemia and reperfusion (Khanal et al., 2011), VGC-rich nascent-bleb membrane should be present well before 2 h since within 2 h of restoring oxygen, balloon-like blebs are evident. Membranes would go through a period of nascent-stage bilayer damage when, it is to be hoped, the insult-induced damage could be arrested and remediated (Draeger et al., 2011). Bilayer injury along these lines is expected with ischemic ATP-depletion, elevated $[Ca^{2+}]_{int}$, free radicals, mechanical trauma, and inflammatory conditions, as well as where various genetic or toxic conditions damaged the cortical cytoskeleton (Allen et al., 2010; McGinn et al., 2009).

Our findings for Nav1.6 channels (Wang et al., 2009) crystallized our realization that while bleb-inducing stretch injury to cell-attached patches acts irreversibly, the consequences for Nav gating are in the same category as those elicited reversibly by elastic stretch. A simple explanation: both blebbing and reversible stretch result in increased disorder/fluidity in the hydrophobic region of the bilayer (Morris, 2011a). In principle, at two extremes, a bilayer deformation could be fully reversible (elastic) or entirely irreversible (plastic). For plasma membrane bilayers, given their complex make-up, progressive change between the two extremes is to be expected.

Fig. 1 schematizes this both for VGCs that make MS-Speed responses and for VGCs that make MS-Number responses; these terms will be further elucidated as we go along. Fig. 1 indicates that in experiments in which $g(V)$ curves (see legend) are monitored before, during and after an imposed stretch, deformations would initially be mostly plastic and eventually fully elastic. "Before, during and after" (see the figure) could refer not only to stretch perturbations but to any insult or process that restructures/perverts the bilayer. Were a membrane simply a symmetric artificial

bilayer, stretch deformations could be fully elastic. But with biological structural complexity, plastic change is unavoidable with stretch. Specifically, for complex biomembranes like the cardiac or oocyte sarcolemma, pipette aspiration experiments will cause blebbing during the plastic-regime, i.e., de-adhesion of bilayer from long-range membrane cytoskeleton structures, accompanied by decreasing leaflet asymmetry and decay of normal laterally-organized domains (Sheetz et al., 2006).

Biomembranes under abrupt or steady mild pipette aspiration will thus progress through a plastic deformation regime. This would explain the progressive, graded, irreversible stretch-induced $g_{Na}(V)$ left-shift of Nav channels in stretched membranes (Tabarean et al., 1999; Wang et al., 2009; Beyder et al., 2010; Morris, 2011a, Morris et al., 2012). At the unitary channel level, it has not been ruled out that what occurs is an all-or-none (i.e., not graded) left-shift process wherein the Nav channel unbinds (or perhaps binds) some putative modulatory ligand (putative candidate are ankyrin-G, actin, syntrophin, sphingomyelin among others, though none have been shown to modulate VGCs as ligands; see Morris et al. (2012)). Whatever the precise left-shift mechanism at the molecular level, irreversible membrane deformations “saturate” at the point when increasingly intense stretch elicits no further irreversible change, and begins to elicit only stretch-intensity dependent elastic responses (Fig. 1). Prior to saturation, plastic changes, should they happen to be large, can easily obscure smaller elastic response components. This occurred in our studies of Nav1.4 (Tabarean et al., 1999); we have now found (unpublished observations) that, like other Nav channels, Nav1.4 shows both plastic and elastic responses to stretch. For Nav1.5 in oocytes, plastic changes happen to be small, allowing elastic behavior to dominate (Banderali et al., 2010b). By contrast, and for reasons not understood, for Nav1.5 in HEK cells, plastic responses appear to dominate (Beyder et al., 2010).

To sum up: a) whatever the bilayer-deforming factor, reversible bilayer perturbations elicit reversible MS modulation of VGCs, while irreversible restructuring elicits irreversible MS modulation, and b) since the physics of elastic (reversible) processes are inherently more explicable than the physics of plastic (irreversible) ones, learning about the reversible responses then determining experimentally if reversible and irreversible MS modulation of VGC-“X” share common features can help in determining if an irreversible and potentially pathological (or physiological) modulation of that VGC species in situ is explained by bilayer perturbations.

4. The MS behavior of VGCs as a matter of the heart – are cardiac bilayers perturbed?

Techniques to study and model tissue mechanics in the beating myocardium are becoming available (e.g. Matsumoto et al., 2012) but their precision and sophistication does not extend to the nanoscale level of bilayer mechanics, the scale relevant for VGCs and other membrane proteins. Whether elastic membrane deformations occur in cardiac membranes on a beat-to-beat basis or more chronically in connection with distended atrial and ventricular chambers is uncertain. Assertions about unidentified stretch-activated cation channels notwithstanding, direct evidence for physiological stretch modulation of any cardiomyocyte ion channel in situ is still lacking, including for the identified and ubiquitous VGCs (Morris, 2011b, 2011c).

Plastic perturbations of cardiac bilayers, on the other hand, are a certainty in relation to dietary lipids, developmental/physiological changes and with various pharmacological agents. Consider a particular VGC species trafficking to both intercalated disc and t-tubular sarcolemmal membranes (Domínguez et al., 2008); at the

different loci it will likely find itself embedded in mechanically-different bilayer structures. Likewise for any particular VGC species in caveolar vs non-caveolar bilayer or in raft vs non-raft bilayer (Kaiser et al., 2009).

Regarding injury-induced irreversible (plastic) changes in bilayer structure that might follow ischemia, inflammation, trauma, exposure to various toxins (Allen et al., 2010; Armstrong et al., 2001; Novak et al., 2009; Post et al., 1988; Haeseler et al., 2008; Klöckner et al., 2011) and so on, the existence of plastic bilayer perturbations is not at issue, but nanoscale information about the specifics is sparse. An exception is a recent study involving rat cardiomyocytes and using laurdan and 1,6-diphenyl-1,3,5-hexatriene to probe membrane fluidity changes (Vadhana et al., 2011) associated with toxic metabolites of pyrethroids. These compounds, which impair VGC function, foster lipid peroxidation of plasmalemmal bilayers. Laurdan, whose fluorescence is sensitive to the extent of water penetration into the bilayer’s hydrophobic interior, probes the lateral mobility and polarity of its environment, while the 1,6-diphenyl-1,3,5-hexatriene measures fluidity changes in the bilayer’s hydrophobic interior; low levels of metabolites (10–20 μ M range) alter membrane fluidity in proportion to metabolite partition coefficients. Using 2-photon microscopy, laurdan signals can be monitored at small depths into living tissues (Owen et al., 2011) (e.g., zebrafish embryos). It might be feasible to monitor mechanically induced changes using fluorescent probes of bilayer structure during ischemia, *comotio cordis* experiments (Kalin et al., 2011), exposure to short-chain alkanols, stretch, and so on.

5. MS-speed and MS-number

5.1. MS kits for putting MS-modulated VGCs into cardiac models

Be they elastic or plastic, bilayer perturbations can accelerate the major depolarization-induced motions of voltage sensors (Laitko and Morris, 2004; Schmidt and MacKinnon, 2008; Morris, 2011b). But voltage sensor movements are several steps removed from the physiological “currency” of excitable cells, namely the flux of ions through open pores, fluxes that charge/discharge V_m and that can mediate $\Delta[Ca^{2+}]_{int}$. Typically, mathematical models of cardiac electrophysiology have as outputs V_m and $[Ca^{2+}]_{int}$ and while unidentified stretch-activated channels are sometimes included in those models (Trayanova et al., 2010), only one preliminary study (Banderali et al., 2010a) recognizes that the ubiquitous VGCs may experience MS modulation (Morris, 2011c). The possibility of pathological MS modulation of VGCs provides a particularly strong argument for incorporating MS-modulated VGC behaviors when modeling arrhythmias.

To a first approximation, the MS modulation falls into the two categories, MS-Speed (e.g., Nav and Kv1 channels: currents accelerate, $g(V)$ shifts leftward along the V_m axis, its slope is fixed, and so too is g_{max}) and MS-Number (e.g., VGCa and Kv3 channels: current speed and $g(V)$ midpoint and slope are unaffected but apparent g_{max} increases). These simple descriptors could help incorporate into cardiac models of electro-rhythmicity, realistic but computationally tractable descriptions of MS-modulated VGCs. The MS-Speed approach we used for Nav channels and axon damage (Boucher et al., 2012) could be modified appropriately for use in cardiac models. For Cav channel leak, a MS-Number approach would be simple. The next section introduces several over-arching concepts to help with computational tool-kits for VGCs in damaged or in otherwise perturbed bilayers. We then discuss these concepts with reference to the MS behavior of a particularly uncomplicated VGC, namely Kv3 (Laitko et al., 2006). Kv3 is doubly useful in the present context: it has VGCa-like MS responses (Morris and Laitko, 2005), and it provides a straightforward way to address the issue of VGC

mode-switching, a class of transitions not to be ignored when studying MS modulation of VGCs. VGC mode-switching is thought to occur beat-to-beat in the myocardium (Männikkö et al., 2005; Karoly et al., 2010). We encountered the complexities of mode-switch in studying MS modulation of HCN2 (Lin et al., 2007) and Nav1.6 (Morris et al., 2012). Unlike Nav (Maltsev and Undrovinas, 2008; and Karoly et al., 2010) and HCN2 (Männikkö et al., 2005) channels, the kinetic simplicity of Kv3 currents makes it possible, from direct inspection of current records, to grasp the idea of mode-switch, without/with stretch modulation of the currents.

5.2. MS-Speed versus MS-Number modulated VGCs: some key concepts

5.2.1. Rate-limiting voltage-dependent (RLVD) transitions

Along the activation pathway of any VGC, there will be a RLVD transition governing the rate of channel opening at a given voltage: that RLVD step may or may not be a MS step. The RLVD step is MS in Nav channels but not in Kv3 or L-type Cav channels (MS kinetics of VGC channels are reviewed in Morris and Laitko (2005)). This, in essence, underlies the MS-Speed and MS-Number categories. Given the complexity of VGC kinetic schemes, these are useful, though not “iron-clad”, descriptors for MS modulation.

5.2.2. Mode-switch

During prolonged depolarizations and hyperpolarizations (e.g. several tens of milliseconds) VGCs (having accomplished their voltage-dependent transitions) undergo voltage-independent mode-switch transitions (Männikkö et al., 2005; Lin et al., 2007; Haddad and Blunck, 2011); the possibility that some mode-switch transitions are MS needs to be investigated.

5.2.3. Chronic MS modulation

Reversible and irreversible responses of VGCs to stretch are qualitatively so similar for Nav channels that a common explanation may suffice. With elastic bilayer stretch, bilayer packing-order decreases; for multi-component bilayers, this is like an entropic softening (Phillips et al., 2009; Bruno et al., 2007; Ingólfsson, and Andersen, 2011). This type of bilayer elasticity modulus change would facilitate lipid repacking at the channel/lipid interface, helping compensate for any stretch-thinning related hydrophobic mismatch, while still facilitating sensor motions (Krepkiy et al., 2009; Finol-Urdaneta et al., 2010). Further studies are needed to establish the generality – or not – of reversible/irreversible response similarities in the MS modulation of VGCs. If this pattern holds then, as with Nav channels, studies on the tractable physics of reversible responses will serve the deeper understanding of plastic (irreversible) responses associated with chronic bilayer perturbations, i.e., those occurring with pathological and developmental membrane changes.

6. Kv3, a MS-speed modulated VGC

6.1. A special rate-limiting voltage-dependent step and the MS response of Kv3

Kv3 channels, like L-type Ca channels, exhibit MS-Number behavior (MS VGCa channel behaviors are reviewed in Morris and Laitko (2005)). Unlike Kv3, $I_{Ca}(V_m, t)$ cannot be studied in stretched oocyte membranes (Calabrese et al., 2002) because lanthanide ions used to inhibit endogenous MS channels block g_{Ca} . Initially, however, we examined Kv3 (Laitko et al., 2006) expecting it to echo the interesting MS-Speed responses of Shaker-ILT, a biophysical-tool Kv1 channel.

Unlike Shaker-Kv1, with its 4th order activation (like Hodgkin–Huxley delayed rectification), Kv3 activation, which requires strongly depolarized potentials, follows 1st order activation kinetics (Ledwell and Aldrich, 1999). These Shaw-Kv3 features inspired the useful Shaker-Kv1 mutant, Shaker-ILT (Lacroix and Bezanilla, 2011; Pathak et al., 2005; del Camino et al., 2005). In Kv1-ILT, voltage sensors are subtly altered by introducing a three amino acid motif, ILT (isoleucine, leucine, threonine) from the Kv3 voltage sensor (Ledwell and Aldrich, 1999). The impact is powerful. In Kv1-WT, gate-charge moves concertedly (simultaneously in 4 subunits) as a 1st order process at about the same only-slightly depolarized voltage as the major sensor-charge movements (4 subunits independently). In Kv1-ILT, however, sensor-charge and gate-charge motions are energetically de-coupled: sensor-charge moves as before, but the concerted movement of gate-charge now requires a strong depolarization; in Kv1-ILT, the concerted gate-motion is the RLVD step governing $P_{open}(t)$.

We have reported on the MS-Number responses of Kv3 (specifically, Kv3-F335A, Laitko et al., 2006), and here include further information for WT, F335A and P410A; this shows the illustrated behaviors to be robust Kv3 characteristics. We focus on amplitudes and time courses of Kv3 currents during and after prolonged depolarizations. Methods were reported previously and data shown here were obtained along with data in the 2006 Laitko et al. paper, where it is explained that these Kv3 mutants are ones studied by the Covarubbias group for their alcohol-modulated gating behaviors, with Kv3-F335A as their experimental-“WT” (Shahidullah et al., 2003; Harris et al., 2003). Reversibly upon stretch, Kv3-F335A P_{open} increases. Unitary currents are unchanged but there is an apparent g_{max} increase with no change in activation speed or other evidence of a $g(V)$ shift (Laitko et al., 2006). Contrast this with Shaker-ILT: reversibly with stretch, its current decelerates and $g(V)$ right-shifts (with g_{max} fixed and slope unchanged) (Laitko et al., 2006). Kv1-ILT and Kv3 both have a late concerted RLVD step, but their MS responses are radically different (MS-Speed vs MS-Number responses), hence a late concerted RLVD step is not a requirement for MS-Number responses. The next section looks further at MS-Number modulation in Kv3.

6.2. More Kv3 MS results – recording conditions

The data in Fig. 3 and Fig. 4 are described in their legends then discussed here. Kv3 cDNAs were kindly provided by M. Covarubbias (see Shahidullah et al. (2003); Harris et al. (2003); Laitko et al. (2006)). Channels were expressed in oocytes at levels sufficient for macroscopic I_K in well-fire-polished (molten soda glass-coated filament) cell-attached patches (Morris et al., 2006). Pipette resistances were 2–4 M Ω . The same high-K⁺ solution (see Lin et al. (2007)) was used for bath and pipette, with 1 mM lanthanum in the pipette to inhibit endogenous channels. Pipette pressures were monitored as before. Linear subtraction of leak and capacitive currents was performed as previously using 4 hyperpolarizing steps in a P/N protocol (Laitko et al., 2006). Unlike experiments on Nav1.6 (Wang et al., 2009) which were done starting with gently-sealed patches (a procedure explained in Morris et al. (2006)), the Kv3 experiments were done on patches sealed using ~10–40 mmHg suction. The patched membranes had probably completed most of their plastic-regime (blebbing) damage by the point recordings began. In retrospect, for these MS-Number channels, any initial plastic damage behavior that would have been evident had we used gently-sealed patches would probably have been interpreted by us as a mysterious and annoying “run-up” (assorted forms of run-up plague whole-cell recording of VGCs). In the Sachs lab, the longstanding term for applying suction to take

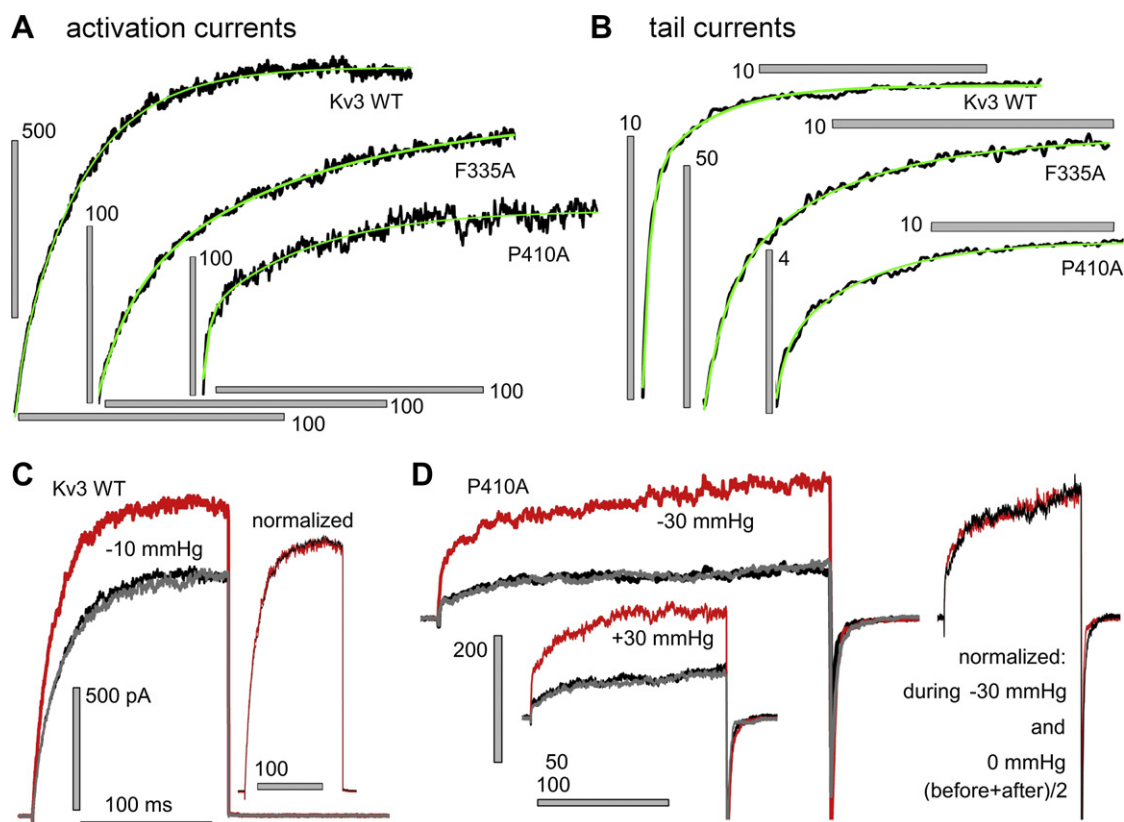


Fig. 3. Kv3 channel kinetics without and with stretch: two open states and MS-Number responses. A, B Typical activation and tail current traces (no stretch) for three Shaw Kv3 channels (WT, F335A and P410A) with overlaid fits (green) for sums of two exponentials. C, D For WT and P410A, traces before/during/after stretch (black, red, gray) and at right for each, the average of before + after traces amplitude-normalized to the during-stretch trace. The complete overlap signifies that stretch had no effect on I_K kinetics. What changes with stretch is the number of channels participating. This Kv3 response to stretch might be comparable to the cardiac L-type VGCa channels facilitating response to pre-pulse depolarization (Costantin et al., 1998) which, by increasing coupling efficacy between sensor movement and pore opening, increases apparent g_{max} with no change in I_{Ca} kinetics.

a patch through its plastic-regime changes is the “exercise protocol” used, for example, to get past MS run-up of cation and TREK channels (Suchyna et al., 2009).

A cautionary note, therefore: run-ups of amplitude and $g(V)$ midpoints of VGCs in patch recordings (and in whole cell recordings where cells inflate (see Calabrese et al. (2002), and Langton (1993)) might reflect temporally and mechanically, bleb-type deterioration of plasma membrane structures.

6.3. Mode-switch – Kv3 fits the pattern

For WT Kv3 and the two point-mutants, Fig. 3A illustrates that upon prolonged depolarizing steps from -100 mV, the 150 ms I_K traces are well-described by the sum of two first order exponentials. As expected (Ledwell and Aldrich, 1999), the first ~ 10 ms of the trace is well fit by a single exponential. However, to fit the 150 ms long current activation traces, sums of two exponentials were required. The Kv3 tail currents (upon repolarization after 150 ms) moreover, followed a two-exponential decay process (Fig. 3B) in all the Kv3 channel variants. This two-exponential pattern of activation/deactivation was invariably observed during 150 ms pulses in these channels.

During prolonged depolarizations, channels can enter a second open state, though this is not evident during the brief (10 ms) standard depolarizations (Ledwell and Aldrich, 1999). The double exponential patterns of activation/deactivation (Fig. 3) would be consistent with the mode-switch scheme sketched in Fig. 5A. This scheme is based on the Active-Mode/Relaxed-Mode model proposed by Bezanilla and colleagues, who emphasize its general

applicability for all VG proteins (Villalba-Galea et al., 2008), VG phosphatases (Villalba-Galea et al., 2008), HCN channels (Männikkö et al., 2005) and Nav channels (Lenkey et al., 2011; Morris et al., 2012) and Kv1 (Haddad and Blunck, 2011), e.g., all exhibit voltage dependent (VD) activation/deactivation and voltage-independent (VI) mode-switch behaviors along this line. Such mode-switching in action in a cardiac physiology context has been modeled for sinoatrial cell rhythms (Männikkö et al., 2005) and our ramp current data for HCN2 channels before/during and after stretch (Fig. 5Biii) (Lin et al., 2007) show that hysteresis (a manifestation of mode-switching (Männikkö et al., 2005) is not abolished by stretch.

We prefer the term “mode-SWITCH” to mode-shift (Lin et al., 2007; Morris et al., 2012). Switch better evokes a discrete conformation change in the voltage-sensor (i.e., a VI transition or “switch” from Active-Mode to Relaxed-Mode or vice versa). When an open Kv or Nav channel (or, for an HCN channel, closed) in Active-Mode mode-switches, it enters a lower energy Relaxed-Mode state (Villalba-Galea et al., 2008). Haddad and Blunck (2011) explain mode-switch as follows: “a mechanical load ... imposed upon the voltage sensors by the pore domain ... allosterically modulates its conformation. Mode shift [switch] is caused by the stabilization of the open state but leads to a conformational change in the voltage sensor.”

The Fig. 5A scheme posits that in hyperpolarized membranes, Kv3 channels would mostly be in a C_A state, whereas with prolonged large depolarizations, O_R would dominate. Steady-state I_{Kv3} during prolonged depolarizations would thus represent some mix of O_R and O_A . The double exponential tail currents are most simply

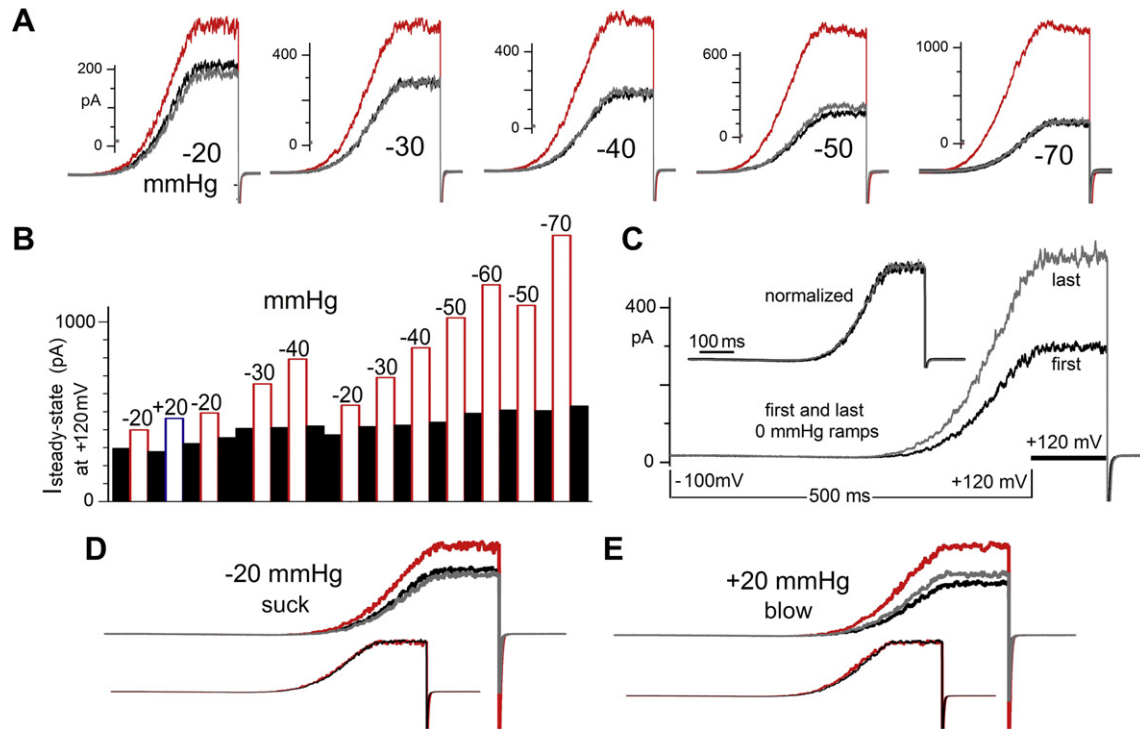


Fig. 4. MS-Number behavior in Shaw Kv3 F335A using ramp-then-hold clamp. A, A series of before/during/after stretch traces, with stretch imposed by pipette aspiration (suction) at the intensities shown (mmHg). The voltage protocol: from $V_{\text{hold}} = -100$ mV, a 500 ms ramp to ± 120 mV and after 120 ms there, back to V_{hold} . (panel C labels these). Note that the I_K plateaus do *not* represent a g_{max} condition, but a steady-state I_K at $+120$ mV (i.e. the y-axis entries in B). Note different current scales. For ~ -40 mm Hg and beyond, stretch-modulated I_K exceeds the depolarization-induced I_K . B, bar diagram summarizing the “stretch-dose” response experiment from which traces in A are taken, with black = 0 mm Hg controls. In C, the first and last 0 mm Hg traces are plotted then normalized (procedure as in Fig. 3), and in D, E the full traces for -20 mm Hg (first time) and $+20$ mm Hg are plotted (with their before and after traces) then normalized. This illustrates MS-Number behavior as seen for ramp-then-hold currents and shows that blowing into the pipette is the equivalent of applying suction, as expected if increased membrane tension underlies the response.

interpreted as reflecting different rates closing (deactivating) from each of the two open states. As with the dual activation process, the dual deactivation processes showed no evidence of a rate change during stretch.

To learn how bilayer perturbations modulate VGCs, it could be useful to determine how the Kv3 transitions governing these currents avoid feeling the reversible membrane deformations due to stretch. It is clear, after all, that as for VGCa channels, Kv3 channels have at least one MS non-rate-limiting voltage-dependent transition along their activation pathway (Calabrese et al., 2002; Laitko et al., 2006).

6.4. An aside on “sites”: chemical and physical MS modulation of Kv3 and other VGCs

In oocyte membranes, inhibition of steady-state I_{Kv3} has been examined for short chain 1-alkanols (Shahidullah et al., 2003). Short chain alkanols cause chain-length dependent bilayer thinning, increased bilayer disorder and reduced surface tension (Ly and Longo, 2004) (for solvent-containing bilayers, see Finol-Urdaneta et al. (2010)). They govern steady-state Kv3 P_{open} in accordance with this pattern, without dose-saturation or stereospecificity (Shahidullah et al., 2003). Kv3 channels unquestionably

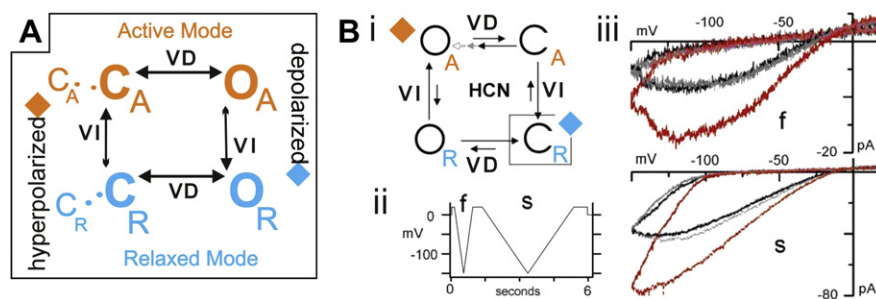


Fig. 5. Mode-switch and MS modulation of VGCs. A, simplified scheme for Kv3 channels in closed/open (C, O) active/relaxed (A, R) mode states connected by voltage-dependent (VD) and voltage-independent (VI) transitions (the latter being the putative mode-switch transitions). In Kv3, additional VD transitions (with voltage sensor motions) must occur between closed states indicated to the left of the scheme, but they are not the rate-limiting transition for pore opening. At least one of those hidden transitions must be a MS transition that, with stretch, augments the fraction of channels “ready-to-open-upon-depolarization”. This scheme is analogous to the mode-switch scheme used for HCN2 channels (Lin et al., 2007), which is redrawn in Bi using the naming and color conventions of A. For both schemes, prolonged hyperpolarization causes channels to populate states near the orange diamond while prolonged depolarization populates states near the blue diamond. Bii, iii illustrate the double-sawtooth ramp protocol (first a fast, f, then a slower, s, voltage sawtooth) used with HCN2 to elicit the characteristic mode-switch-induced I_{cation} hysteresis before, during, after stretch (modified from Lin et al. (2007)).

feel bilayer perturbations (Laitko et al., 2006) yet this is ignored in models that view alcohols and general anesthetics solely as ligands acting at specific protein-based binding sites (Barber et al., 2011). If alcohols indeed destabilize the Kv3 open state (two states, in fact, as seen here) via allosteric actions at an entirely protein-based binding site, the MS entity being modulated nevertheless resides in an alcohol-perturbed bilayer structure (Finol-Urdaneta et al., 2010; Ingólfsson, and Andersen, 2011). As stressed by the Mackinnon group (Schmidt and MacKinnon, 2008; Schmidt et al., 2009) models should factor in all bilayer constituents when considering the energetics of P_{open} (or, as here, $P_{(O_A+O_R)}$). For lipidic constituents present in sufficient quantity to perturb the peri-VGC bilayer structure, for countless amphiphilic drugs that produce VGC side effects, MS modulation is a more plausible explanation than low affinity binding at hydrophobic “sites” or “pockets” (see Morris and Juranka (2007b), Finol-Urdaneta et al. (2010), Rusinova et al. (2011)). It is useful to envisage MS modulation in the following way: the entire structured lateral interface between VGCs and the bilayer leaflets (Phillips et al., 2009) is in effect an “allosteric effector site” for VGC motions (Morris, 2011a).

6.5. Rate-limiting voltage dependent steps: is the RLVD transition an MS transition?

Among different VGC species, the precise ways in which voltage sensor motions regulate ion-current flow differ. By definition, any motion of a voltage sensor through the electric field will be voltage-dependent (VD) and where a VD sensor motion also “feels bilayer deformations, it will be a MS-VD motion. However, part of a sensor’s total VD movement could occur buried in the protein in a way that rendered it insensitive to bilayer deformations. This serves as a generic explanation for why the RLVD activation step in Kv3 and Cav channels (Calabrese et al., 2002) is not a MS transition. In Fig. 5A, the Kv3 channel MS transition(s) would lie somewhere on the left (i.e., as viewed by ionic current, they would be hidden Markov transitions (Morris and Juranka, 2007b) in the “ C_A – C_A ” and/or “ C_R – C_R ” zone). A VGC could also have MS-VI transitions. Slow inactivation (presumably P/C-type) in Shaker Kv1-5aa is an example (Laitko and Morris, 2004) and anomalous mode-conversion in α Nav1.4 (Tabarean et al., 1999; Shcherbatko et al., 1999) is a possible candidate for a MS-VI mode-switch transition.

Thus, the slowest VD step along the path to “open” – the RLVD step – may or may not be a MS step. For VGCs whose RLVD step is a MS step, bilayer deformations will accelerate (as in Nav1.5 (Banderali et al., 2010b) or decelerate (as in Kv1-ILT) activation, thereby left- or right-shifting $g(V)$. When the bilayer surround of say, a Nav channel, is reversibly disordered/thinned/fluidized (by stretch, by fluidizing agents), $I_{\text{Na}}(t)$ reversibly accelerates for all values of V_m (e.g. Fig. 1C of Morris and Juranka (2007a)) and Fig. 3D of Banderali et al. (2010b) show stretch-accelerated activation at V_m levels where g_{max} has already been attained). But for an L-type Cav channel, whose RLVD step (like that of Kv3) is a non-MS transition, $I_{\text{Ca}}(t)$ for all values of V_m scales up by the same amount. This translates to apparent g_{max} increasing by that scaling factor. The mechanosensitivity (or not) of the RLVD transition thus provides a general explanation for the two categories of MS modulated VGC behavior, “MS-Speed” and “MS-Number”.

7. Similarities in reversible and irreversible MS responses: from biophysics to pathology

Reversible stretch modulation of VGCs signifies elastic changes in bilayer structure (Gu et al., 2001; Tabarean and Morris, 2002;

Lin et al., 2007; Morris and Juranka, 2007a), but assigning mechanisms for irreversible stretch-modulation is more difficult (Tabarean et al., 1999; Shcherbatko et al., 1999; Morris et al., 2006; Suchyna et al., 2009). However, pipette aspiration is useful because stretch first causes progressive blebbing damage then saturation is achieved and bilayer deformations thereafter are elastic (Morris and Horn, 1991; Small and Morris, 1994; Wan et al., 1999; Morris, 2011a; Zhang et al., 2000; Sheetz et al., 2006; Suchyna et al., 2009). Nav1.6 currents in oocyte patches exemplify the plastic then elastic MS-Speed diagram of Fig. 1 (see Fig. 5 in Wang et al., 2009).

The equivalent plastic–elastic diagram for MS-Number channels in Fig. 1 is in agreement with N-type Cav channels in HEK cells (Calabrese et al., 2002). Concomitant I_{Ca} and video imaging of the whole-cell inflation process revealed that MS-Number responses (increased apparent g_{max} , unchanged $I_{\text{Ca}}(t)$ activation rise time) occurred when the positive pressure abruptly caused blebbing inflation damage. Unitary channel recordings from cell-attached patches (the small tips needed for large gigaohm seals unavoidably damaged the patched membranes) showed that stretch elicited reversible “ iNP_{open} ” increases of the same magnitude obtained by whole-cell inflation. Unitary event analysis indicated that the increase was attributable to increased N (number of participating channels), not to increased unitary current (i) or to a changed unitary event open duration. For these N-type VGCa channels, therefore, the plastic–elastic diagram seems appropriate, though monitoring the gradual progress of plastic regime damage was not possible in the HEK cell preparation.

Ionic and gating currents of cardiac L-type Cav channels (cut-open oocyte recordings) reveal that the coupling efficacy between voltage sensor charge movement and pore opening in these channels is facilitated by prolonged prepulse depolarizations (Costantin et al., 1998), with no change in $I_{\text{Ca}}(t)$ kinetics. In other words, apparent g_{max} increases with prepulse depolarizations. Sustained membrane stretch mimics the effect of the prepulse depolarization.

Leaky Cav channels (and ryanodine receptors) in ischemically damaged cardiomyocytes are important drug targets (Hu et al., 2011; Fauconnier et al., 2011). For those concerned with the underlying mechanisms of Cav-leak, a key question, we suggest, is this: does blebbing membrane damage of cardiomyocyte membrane elicit an irreversible increase in apparent g_{max} ? Assume it does (and many lines of evidence suggests it does, if whole cell-clamp cell-inflation data for L-type Cav currents are interpreted as *damage-augmented* I_{Ca} ; see VGCa section in Morris and Laitko (2005)) and assume the facilitation mechanism identified by Costantin et al. (1998) is involved. In that case fluidizing perturbations to the cut-open oocyte membrane should irreversibly left-shift the gating charge curve ($Q(V)$), a testable idea. The outcome: a highly undesirable (irreversible, i.e., leak) version of the “facilitation” normally elicited by long depolarizations.

Consider cardiac Nav1.5 in rat ventricular myocytes where, in spite of difficulty forming and maintaining patches, we demonstrated that Nav1.5 exhibits elastic MS-Speed behavior (Banderali et al., 2010a). In HEK cells Beyder et al. (2010) found that Nav1.5 channels under patch-stretch show plastic MS-Speed responses. It is reasonable, therefore, to predict that Nav1.5 (slow- and fast-gating) in native membranes experiencing blebbing injury (from ischemia, from inflammation, abrupt mechanical insults) would develop MS-Speed type Nav-leak.

In oocyte patches, the Kv3 MS-Number responses were largely reversible (as mentioned above, non-gentle procedures were used to form the patches). Nevertheless, such irreversible change as occurred followed the MS-Number elastic response pattern, as illustrated by Fig. 4. For that patch, currents (A) were repeatedly

acquired without/with stretch (suction or blowing) until the patch ruptured, as summarized in B. Applied pressure over a wide range of doses reversibly increased apparent g_{\max} in a “dose” dependent fashion expected when membrane tension is the effective mechanical stimulus. And, consistent with the MS-Number responses showing no effect of stretch on activation and deactivation time courses (Fig. 3)), the normalized $I_K(t)$ for the Fig. 4 ramp-then-hold traces (without/with stretch) superimpose perfectly. However, as evident from the generally “upward” trend of 0 mm Hg control current in the bar diagram, apparent g_{\max} at 0 mm Hg almost doubled. This trend might represent a gradual irreversible doubling of the patch area (unlikely given that linear subtraction remained excellent throughout, with no readjustments once the experiment started), or it might be a Kv3 version of Cav channel-like run-up. If this indeed represents a plastic change, then it is noteworthy that the normalized I/V traces for the first and last 0 mm Hg ramps overlap perfectly (Fig. 4C), mechanistically consistent with the elastic-regime MS-Number response. This unquestionably anecdotal datum is included because it could serve as a helpful template for re-visiting ischemic membrane damage in cardiomyocyte L-type Ca channels (Du and Nathan, 2007). In those clinically pivotal channels, damage-linked I_{Ca} run-up could easily signify a dangerous irreversible MS-Number response, that is, a Cav-leak caused by the irreversibly perturbed bilayer structure.

8. Conclusions

VGCs are multi-conformation membrane proteins. Their voltage sensors interact extensively with the embedding bilayer and so, in order to repack during conformation changes, must do work on the bilayer. VGCs thus cannot both gate and remain entirely indifferent to the mechanical state of their bilayer. In the myocardium, where VGCs see a continually changing V_m , the default assumption should be that inappropriate bilayer perturbations will be pro-arrhythmic.

If a bilayer becomes more fluid/disorderly/thin/poorly-packed, voltage sensors will move more easily. In principle, a bilayer might alternate reversibly (in an elastic fashion) or irreversibly (in a plastic fashion) between this and the opposite extreme. VGCs will respond reversibly or irreversibly, as the situation demands. Because the many species of VGCs couple their sensor motions to gate opening in different ways, however, responses to perturbed bilayer structure plays out differently in different VGCs. For most VGCs, this simplifies to saying that either a) activation of some fixed population of channels speeds up or b) that the population of channels opening at some fixed speed increases.

Plastic bilayer perturbations occur in cardiomyocytes subjected to ischemic, inflammatory and other conditions. For axonal Nav channels, we showed that taking the plastic changes seriously in the context of mild axon damage yields ectopic firing patterns typical of peripheral neuropathies.

We hope our characterization of MS-modulation of diverse VGCs into two categories will help cardiac experimentalists and modelers re-examine the “leaky” VGCs of acquired cardiac disease states. We suggest how to determine if they are in fact manifesting MS-modulation. This should urgently be re-addressed for VGNa and VGCa channels.

Many clinically promising or useful VGC inhibitors are lipophilic (Mason, 1993; Lenkey et al., 2011; Karoly et al., 2010). As such, they might partition more poorly into healthy, well-packed bilayers than into damaged-fluidized (blebbing) bilayers. Where the leaky VGCs targeted by lipophilic inhibitors are channels experiencing MS-modulation in damaged bilayers, there could be opportunities to optimize targeting. To reduce unwanted inhibition of non-leaky VGCs in healthy membrane, the drug could be modified to ensure

that its specific binding to the VGC-site is most effective in perturbed bilayers. Further, increasing the drug’s partition co-efficient for fluidized (relative to healthy) VGC-rich bilayers would also enhance selectivity. In a perverse fashion, nature seems to take this general approach in spider venoms, where toxic amphiphilic peptides are accompanied by membrane-fluidizing lipases. The toxic peptides target binding sites on voltage sensors, but their efficacy as VGC inhibitors is greatly improved when the embedding bilayer becomes fluidized (Schmidt and MacKinnon, 2008; Morris, 2011b; Morris et al., 2012).

Acknowledgments

The authors acknowledge funding from CIHR (CEM) and NSERC (BJ).

References

- Ali, M.H., Kirby, D.J., Mohammed, A.R., Perrie, Y., 2010. Solubilisation of drugs within liposomal bilayers: alternatives to cholesterol as a membrane stabilising agent. *J. Pharm. Pharmacol.* 62, 1646–1655.
- Allen, D.G., Zhang, B.T., Whitehead, N.P., 2010. Stretch-induced membrane damage in muscle: comparison of wild-type and mdx mice. *Adv. Exp. Med. Biol.* 682, 297–313.
- Armstrong, S.C., Latham, C.A., Shivell, C.L., Ganote, C.E., 2001. Ischemic loss of sarcolemmal dystrophin and spectrin: correlation with myocardial injury. *J. Mol. Cell. Cardiol.* 33, 1165–1179.
- Banderali, U., Clark, R.B., Morris, C.E., Fink, M., Giles, W.R., 2010a. Effects of applied stretch on native and recombinant cardiac Na^+ currents. In: Kamkin, A., Kiseleva, I. (Eds.), *Mechanosensitivity in Cells and Tissues: Mechanosensitivity of the Heart*. Springer, pp. 169–184.
- Banderali, U., Juranka, P.F., Clark, R.B., Giles, W.R., Morris, C.E., 2010b. Impaired stretch modulation in potentially lethal cardiac sodium channel mutants. *Channels (Austin)* 4, 12–21.
- Barber, A.F., Liang, Q., Amaral, C., Treptow, W., Covarrubias, M., 2011. Molecular mapping of general anesthetic sites in a voltage-gated ion channel. *Biophys. J.* 101, 1613–1622.
- Beyder, A., Rae, J.L., Bernard, C., Stregle, P.R., Sachs, F., Farrugia, G., 2010. Mechano-sensitivity of Nav1.5, a voltage-sensitive sodium channel. *J. Physiol.* 588, 4969–4985.
- Bouchard, S., Jacquemet, V., Vinet, A., 2011. Automaticity in acute ischemia: bifurcation analysis of a human ventricular model. *Phys. Rev. E Stat. Nonlin. Soft Matter Phys.* 83, 011911.
- Boucher, P.A., Joós, B., Morris, C.E., 2012 Apr 5. Coupled left-shift of Nav channels: modeling the Na^+ -loading and dysfunctional excitability of damaged axons. *J. Comput. Neurosci.* [Epub ahead of print].
- Bruno, M.J., Koeppe, R.E., Andersen, O.S., 2007. Docosahexaenoic acid alters bilayer elastic properties. *Proc. Natl. Acad. Sci. U S A* 104, 9638–9643.
- Calabrese, B., Tabarean, I.V., Juranka, P., Morris, C.E., 2002. Mechano-sensitivity of N-type calcium channel currents. *Biophys. J.* 83, 2560–2574.
- Charras, G., Paluch, E., 2008. Blebs lead the way: how to migrate without lamellipodia. *Nat. Rev. Mol. Cell. Biol.* 9, 730–736.
- Conti, F., Fioravanti, R., Segal, J.R., Stühmer, W.J., 1982. Pressure dependence of the sodium currents of squid giant axon. *Membr. Biol.* 69, 23–34.
- Costantin, J.L., Qin, N., Zhou, J., Platano, D., Birnbaumer, L., Stefani, E., 1998. Long lasting facilitation of the rabbit cardiac Ca^{2+} channel: correlation with the coupling efficiency between charge movement and pore opening. *FEBS Lett.* 423, 213–217.
- del Camino, D., Kanevsky, M., Yellen, G., 2005. Status of the intracellular gate in the activated-not-open state of shaker K⁺ channels. *J. Gen. Physiol.* 126, 419–428.
- DiFrancesco, D., Borer, J.S., 2007. The funny current: cellular basis for the control of heart rate. *Drugs* 67 (Suppl. 2), 15–24.
- Domínguez, J.N., de la Rosa, A., Navarro, F., Franco, D., Aránega, A.E., 2008. Tissue distribution and subcellular localization of the cardiac sodium channel during mouse heart development. *Cardiovasc. Res.* 78, 45–52.
- Draeger, A., Monastyrskaya, K., Babychuk, E.B., 2011. Plasma membrane repair and cellular damage control: the annexin survival kit. *Biochem. Pharmacol.* 81, 703–712.
- Du, Y.M., Nathan, R.D., 2007. Simulated ischemia enhances L-type calcium current in pacemaker cells isolated from the rabbit sinoatrial node. *Am. J. Physiol. Heart Circ. Physiol.* 293, H2986–H2994.
- Fauconnier, J., Meli, A.C., Thireau, J., Roberge, S., Shan, J., Sassi, Y., Reiken, S.R., Rauzier, J.M., Marchand, A., Chauvier, D., Cassan, C., Crozier, C., Bideaux, P., Lompré, A.M., Jacotot, E., Marks, A.R., Lacampagne, A., 2011. Ryanodine receptor leak mediated by caspase-8 activation leads to left ventricular injury after myocardial ischemia-reperfusion. *Proc. Natl. Acad. Sci. U S A* 108, 13258–13263.
- Finol-Urdaneta, R.K., McArthur, J.R., Juranka, P.F., French, R.J., Morris, C.E., 2010. Modulation of KvAP unitary conductance and gating by 1-alkanols and other surface active agents. *Biophys. J.* 98, 762–772.

- Ganapathi, S.B., Fox, T.E., Kester, M., Elmslie, K.S., 2010. Ceramide modulates HERG potassium channel gating by translocation into lipid rafts. *Am. J. Physiol. Cell. Physiol.* 299, C74–C86.
- Gu, C.X., Juranka, P.F., Morris, C.E., 2001. Stretch-activation and stretch-inactivation of Shaker-IR, a voltage-gated K⁺ channel. *Biophys. J.* 80, 2678–2693.
- Haddad, G.A., Blunck, R., 2011. Mode shift of the voltage sensors in Shaker K⁺ channels is caused by energetic coupling to the pore domain. *J. Gen. Physiol.* 137, 455–472.
- Haeseler, G., Foadi, N., Wiegand, E., Ahrens, J., Krampfl, K., Dengler, R., Leuwer, M., 2008. Endotoxin reduces availability of voltage-gated human skeletal muscle sodium channels at depolarized membrane potentials. *Crit. Care Med.* 36, 1239–1247.
- Harris, T., Graber, A.R., Covarrubias, M., 2003. Allosteric modulation of a neuronal K⁺ channel by 1-alkanols is linked to a key residue in the activation gate. *Am. J. Physiol. Cell. Physiol.* 285, C788–C796.
- Hirn, C., Shapovalov, G., Petermann, O., Roulet, E., Ruegg, U.T., 2008. Nav1.4 deregulation in dystrophic skeletal muscle leads to Na⁺ overload and enhanced cell death. *J. Gen. Physiol.* 132, 199–208.
- Hu, X., Wu, B., Wang, X., Xu, C., He, B., Cui, B., Lu, Z., Jiang, H., 2011. Minocycline attenuates ischemia-induced ventricular arrhythmias in rats. *Eur. J. Pharmacol.* 654, 274–279.
- Ingólfsson, H.L., Andersen, O.S., 2011. Alcohol's effects on lipid bilayer properties. *Biophys. J.* 101, 847–855.
- Kaiser, H.J., Lingwood, D., Levental, I., Sampaio, J.L., Kalvodova, L., Rajendran, L., Simons, K., 2009. Order of lipid phases in model and plasma membranes. *Proc. Natl. Acad. Sci. U S A* 106, 16645–16650.
- Kalin, J., Madias, C., Alsheikh-Ali, A.A., Link, M.S., 2011. Reduced diameter spheres increases the risk of chest blow-induced ventricular fibrillation (commotio cordis). *Heart Rhythm* 8, 1578–1581.
- Karoly, R., Lenkey, N., Juhasz, A.O., Vizi, E.S., Mike, A., 2010. Fast- or slow-inactivated state preference of Na⁺ channel inhibitors: a simulation and experimental study. *PLoS Comput. Biol.* 6, e1000818.
- Khanal, G., Chung, K., Solis-Wever, X., Johnson, B., Pappas, D., 2011. Ischemia/reperfusion injury of primary porcine cardiomyocytes in a low-shear microfluidic culture and analysis device. *Analyst* 136, 3519–3526.
- Klöckner, U., Ruckeschloss, U., Grossmann, C., Ebel, H., Müller-Werdan, U., Loppnow, H., Werdan, K., Gekle, M., 2011. Differential reduction of HCN channel activity by various types of lipopolysaccharide. *Mol. Cell. Cardiol.* 51, 226–235.
- Kovalsky, Y., Amir, R., Devor, M., 2008. Subthreshold oscillations facilitate neuropathic spike discharge by overcoming membrane accommodation. *Exp. Neurol.* 210, 194–206.
- Krepkiy, D., Mihailescu, M., Freites, J.A., Schow, E., Worcester, D., Gawrisch, K., Tobias, D.J., White, S.H., Swartz, K., 2009. Structure and hydration of membranes embedded with voltage-sensing domains. *Nature* 462, 473–479.
- Lacroix, J.J., Bezanilla, F., 2011. Control of a final gating charge transition by a hydrophobic residue in the S2 segment of a K⁺ channel voltage sensor. *Proc. Natl. Acad. Sci. U S A* 108, 6444–6449.
- Laitko, U., Juranka, P.F., Morris, C.E., 2006. Membrane stretch slows the concerted step prior to opening in a Kv channel. *J. Gen. Physiol.* 127, 687–701.
- Laitko, U., Morris, C.E., 2004. Membrane tension accelerates rate-limiting voltage-dependent activation and slow inactivation steps in a Shaker channel. *J. Gen. Physiol.* 123, 135–154.
- Langton, P.D., 1993. Calcium channel currents recorded from isolated myocytes of rat basilar artery are stretch sensitive. *J. Physiol.* 471, 1–11.
- Ledwell, J.L., Aldrich, R.W., 1999. Mutations in the S4 region isolate the final voltage-dependent cooperative step in potassium channel activation. *J. Gen. Physiol.* 113, 389–414.
- Lei, M., Jones, S.A., Liu, J., Lancaster, M.K., Fung, S.S., Dobrzynski, H., Camelliti, P., Maier, S.K., Noble, D., Boyett, M.R., 2004. Requirement of neuronal- and cardiac-type sodium channels for murine sinoatrial node pacemaking. *J. Physiol.* 559, 835–848.
- Lenkey, N., Karoly, R., Epresi, N., Vizi, E., Mike, A., 2011. Binding of sodium channel inhibitors to hyperpolarized and depolarized conformations of the channel. *Neuropharmacology* 60, 191–200.
- Létienne, R., Bel, L., Bessac, A.M., Vacher, B., Le Grand, B., 2009. Myocardial protection by F 15845, a persistent sodium current blocker, in an ischemia-reperfusion model in the pig. *Eur. J. Pharmacol.* 624, 16–22.
- Li, G.R., Sun, H.Y., Zhang, X.H., Cheng, L.C., Chiu, S.W., Tse, H.F., Lau, C.P., 2009. Omega-3 polyunsaturated fatty acids inhibit transient outward and ultrarapid delayed rectifier K⁺ currents and Na⁺ current in human atrial myocytes. *Cardiovasc. Res.* 81, 286–293.
- Lin, W., Laitko, U., Juranka, P.F., Morris, C.E., 2007. Dual stretch responses of mHCN2 pacemaker channels: accelerated activation, accelerated deactivation. *Biophys. J.* 92, 1559–1572.
- Liu, Q., Kong, A.L., Chen, R., Qian, C., Liu, S.W., Sun, B.G., Wang, L.X., Song, L.S., Hong, J., 2011. Propofol and arrhythmias: two sides of the coin. *Acta Pharmacol. Sin* 32, 817–823.
- Ly, H.V., Longo, M.L., 2004. The influence of short-chain alcohols on interfacial tension, mechanical properties, area/molecule, and permeability of fluid lipid bilayers. *Biophys. J.* 87, 1013–1033.
- Maltsev, V.A., Undrovinas, A., 2008. Late sodium current in failing heart: friend or foe? *Prog. Biophys. Mol. Biol.* 96, 421–451.
- Männikkö, R., Pandey, S., Larsson, H.P., Elinder, F., 2005. Hysteresis in the voltage dependence of HCN channels: conversion between two modes affects pacemaker properties. *J. Gen. Physiol.* 125, 305–326.
- Mason, R.P., 1993. Membrane interaction of calcium channel antagonists modulated by cholesterol. Implications for drug activity. *Biochem. Pharmacol.* 45, 2173–2183.
- Matsumoto, K., Tanaka, H., Tatsumi, K., Miyoshi, T., Hiraishi, M., Kaneko, A., Tsuji, T., Ryo, K., Fukuda, Y., Yoshida, A., Kawai, H., Hirata, K.I., 2012. Left ventricular dyssynchrony using three-dimensional speckle-tracking imaging as a determinant of torsional mechanics in patients with idiopathic dilated cardiomyopathy. *Am. J. Cardiol.* Jan 27 (epub).
- McGinn, M.J., Kelley, B.J., Akinyi, L., Oli, M.W., Liu, M.C., Hayes, R.L., Wang, K.K.W., Powlislock, J.T., 2009. Biochemical, structural, and biomarker evidence for calpain-mediated cytoskeletal change after diffuse brain injury uncomplicated by contusion. *J. NeuroPathol. Exp. Neurol.* 68, 241–249.
- Moreno, J.D., Clancy, C.E., 2012. Pathophysiology of the cardiac late Na current and its potential as a drug target. *J. Mol. Cell. Cardiol.* Dec 16 (epub).
- Morris, C.E., 2011a. Why are so many ion channels mechanosensitive. In: Sperelakis, N. (Ed.), *Cell Physiology Source Book*, fourth ed. Elsevier, pp. 493–505.
- Morris, C.E., 2011b. Voltage-gated channel mechanosensitivity. Fact or friction? *Front. Physiol.* 2 (25).
- Morris, C.E., 2011c. Pacemaker, potassium, calcium, sodium: stretch modulation of the voltage-gated channels. In: Kohl, P., Sachs, F., Franz, M.R. (Eds.), *Cardiac Mechano-Electric Coupling and Arrhythmias*, second ed. Oxford University Press, pp. 42–49.
- Morris, C.E., Boucher, P.A., Joós, B., 2012. Left-shifted Nav channels in trauma-damaged bilayer: primary targets for neuroprotective Nav antagonists? *Front. Pharmacol.* 3, 19.
- Morris, C.E., Horn, R., 1991. Failure to elicit neuronal macroscopic mechanosensitive currents anticipated by single-channel studies. *Science* 251, 1246–1249.
- Morris, C.E., Juranka, P.F., 2007a. Nav channel mechanosensitivity: activation and inactivation accelerate reversibly with stretch. *Biophys. J.* 93, 822–833.
- Morris, C.E., Juranka, P.F., 2007b. Lipid stress at play: mechanosensitivity of voltage-gated channels. *Curr. Top. Membranes* 59, 297–337.
- Morris, C.E., Juranka, P.F., Lin, W., Morris, T.J., Laitko, U., 2006. Studying the mechanosensitivity of voltage-gated channels using oocyte patches. *Methods Mol. Biol.* 322, 315–329.
- Morris, C.E., Laitko, U., 2005. The mechanosensitivity of voltage-gated channels may contribute to cardiac mechano-electric feedback. In: Kohl, P., Sachs, F., Franz, M. (Eds.), *Cardiac Mechano-Electric Feedback and Arrhythmias: From Pipette to Patient*. Elsevier Saunders, pp. 33–41.
- Morris, C.E., Sigurdson, W.J., 1989. Stretch-inactivated ion channels coexist with stretch-activated ion channels. *Science* 243, 807–809.
- Mottram, A.R., Valdivia, C.R., Makielski, J.C., 2011. Fatty acids antagonize bupivacaine-induced I_{Na} blockage. *Clin. Toxicol. (Phila.)* 49, 729–733.
- Novak, K.R., Nardelli, P., Cope, T.C., Filatov, G., Glass, J.D., Khan, J., Rich, M.M., 2009. Inactivation of sodium channels underlies reversible neuropathy during critical illness in rats. *J. Clin. Invest.* 119, 1150–1158.
- Owen, D.M., Rentero, C., Magenau, A., Abu-Siniyeh, A., Gaus, K., 2011. Quantitative imaging of membrane lipid order in cells and organisms. *Nat. Protoc.* 7, 24–35.
- Pathak, M., Kurtz, L., Tombola, F., Isacoff, E., 2005. The cooperative voltage sensor motion that gates a potassium channel. *J. Gen. Physiol.* 125, 57–69.
- Periasamy, N., Teichert, H., Weise, K., Vogel, R.F., Winter, R., 2009. Effects of temperature and pressure on the lateral organization of model membranes with functionally reconstituted multidrug transporter LmrA. *Biochim. Biophys. Acta* 1788, 390–401.
- Phillips, R., Ursell, T., Wiggins, P., Sens, P., 2009. Emerging roles for lipids in shaping membrane-protein function. *Nature* 459, 379–385.
- Post, J.A., Ruigrok, T.J., Verkleij, A.J., 1988. Phospholipid reorganization and bilayer destabilization during myocardial ischemia and reperfusion: a hypothesis. *J. Mol. Cell. Cardiol.* 20 (Suppl. 2), 107–111.
- Remme, C.A., Bezzina, C.R., 2010. Sodium channel (dys)function and cardiac arrhythmias. *Cardiovasc. Ther.* 28, 287–294.
- Rusinova, R., Herold, K.F., Sanford, R.L., Greathouse, D.V., Hemmings Jr., H.C., Andersen, O.S., 2011. Thiazolidinedione insulin sensitizers alter lipid bilayer properties and voltage-dependent sodium channel function: implications for drug discovery. *J. Gen. Physiol.* 138, 249–270.
- Sage, M.D., Jennings, R.B., 1988. Cytoskeletal injury and subsarcolemmal bleb formation in dog heart during in vitro total ischemia. *Am. J. Pathol.* 133, 327–337.
- Schafer, D.S., Jha, S., Liu, F., Akella, T., McCullough, L.D., Rasband, M.N., 2009. Disruption of the axon initial segment cytoskeleton is a new mechanism for neuronal injury. *J. Neurosci.* 29, 13242–13254.
- Schmidt, D., Cross, S.R., MacKinnon, R.A., 2009. Gating model for the archeal voltage-dependent K⁺ channel KvAP in DHPc and POPE: POPG decane lipid bilayers. *J. Mol. Biol.* 390, 902–912.
- Schmidt, D., MacKinnon, R., 2008. Voltage-dependent K⁺ channel gating and voltage sensor toxin sensitivity depend on the mechanical state of the lipid membrane. *Proc. Natl. Acad. Sci. U S A* 105, 19276–19281.
- Shahidullah, M., Harris, T., Germann, M.W., Covarrubias, M., 2003. Molecular features of an alcohol binding site in a neuronal potassium channel. *Biochemistry* 42, 11243–11252.
- Shcherbatko, A., Ono, F., Mandel, G., Brehm, P., 1999. Voltage-dependent sodium channel function is regulated through membrane mechanics. *Biophys. J.* 77, 1945–1959.
- Sheetz, M.P., Sable, J.E., Döbereiner, H.G., 2006. Continuous membrane cytoskeleton adhesion requires continuous accommodation to lipid and cytoskeleton dynamics. *Annu. Rev. Biophys. Biomol. Struct.* 35, 417–434.
- Small, D.L., Morris, C.E., 1994. Delayed activation of single mechanosensitive channels in *Lymanea* neurons. *Am. J. Phys.* 267, C598–C606.

- Suchyna, T.M., Markin, V.S., Sachs, F., 2009. Biophysics and structure of the patch and the gigaseal. *Biophys. J.* 97, 738–747.
- Tabarean, I.V., Juranka, P., Morris, C.E., 1999. Membrane stretch affects gating modes of a skeletal muscle sodium channel. *Biophys. J.* 77, 758–774.
- Tabarean, I.V., Morris, C.E., 2002. Membrane stretch accelerates activation and slow inactivation in Shaker channels with S3-S4 linker deletions. *Biophys. J.* 82, 2982–2994.
- Taddese, A., Bean, B.P., 2002. Subthreshold sodium current from rapidly inactivating sodium channels drives spontaneous firing of tuberomammillary neurons. *Neuron* 33, 587–600.
- Trayanova, N.A., Constantino, J., Gurev, V., 2010. Models of stretch-activated ventricular arrhythmias. *J. Electrocardiol.* 43, 479–485.
- Tuazon, M.A., Henderson, G.C., 2012. Fatty acid profile of skeletal muscle phospholipid is altered in mdx mice and is predictive of disease markers. *Metabolism* 61, 801–811.
- Vadhana, D., Carloni, M., Fedeli, D., Nasuti, C., Gabbianelli, R., 2011. Perturbation of rat heart plasma membrane fluidity due to metabolites of permethrin insecticide. *Cardiovasc. Toxicol.* 11, 226–234.
- VanWinkle, W.B., Snuggs, M., Miller, J.C., Buja, L.M., 1994. Cytoskeletal alterations in cultured cardiomyocytes following exposure to the lipid peroxidation product, 4-hydroxynonenal. *Cell. Motil. Cytoskeleton* 28, 119–134.
- Villalba-Galea, C.A., Sandtner, W., Starace, D.M., Bezanilla, F., 2008. S4-based voltage sensors have three major conformations. *Proc. Natl. Acad. Sci. USA* 105, 17600–17607.
- Wan, X., Juranka, P., Morris, C.E., 1999. Activation of mechanosensitive currents in traumatized membrane. *Am. J. Physiol.* 276, C318–C327.
- Wang, J.A., Lin, W., Morris, T., Banderali, U., Juranka, P.F., Morris, C.E., 2009. Membrane trauma and Na⁺ leak from Nav1.6 channels. *Am. J. Physiol. Cell. Physiol.* 297, C823–C834.
- Weiss, S., Benoist, D., White, E., Teng, W., Saint, D.A., 2010. Riluzole protects against cardiac ischaemia and reperfusion damage via block of the persistent sodium current. *Br. J. Pharmacol.* 160, 1072–1082.
- Wolf, J.A., Stys, P.K., Lusardi, T., Meaney, D., Smith, D.H., 2001. Traumatic axonal injury induces calcium influx modulated by tetrodotoxin-sensitive sodium channels. *J. Neurosci.* 21, 1923–1930.
- Yifrach, O., MacKinnon, R., 2002. Energetics of pore opening in a voltage-gated K(+) channel. *Cell* 111, 231–239.
- Yu, N., Morris, C.E., Joós, B., Longtin, A. Spontaneous excitation patterns computed for axons with injury-like impairments of sodium channels and Na/K pumps. *PLoS Comp. Bio.* in press.
- Zhang, Y., Gao, F., Popov, V.L., Wen, J.W., Hamill, O.P., 2000. Mechanically gated channel activity in cytoskeleton-deficient plasma membrane blebs and vesicles from *Xenopus* oocytes. *J. Physiol.* 523, 117–130.